Book Title
Book Editors
IOS Press, 2003

Mutual Localization and 3D Mapping by Cooperative Mobile Robots

Julian Ryde and Huosheng Hu
Department of Computer Science, University of Essex
Wivenhoe Park, Colchester CO4 3SQ, England
E-mail: jryde@essex.ac.uk, hhu@essex.ac.uk

Abstract. This paper describes the development of a 3D laser scanner and an approach to 3D mapping and localization. The 3D scanner consists of a standard 2D laser scanner and a rotating mirror assembly. Employing multiple robots and mutual localization local 3D maps are built. Global localization within the maps is performed by extracting a cross-section of the map just below the ceiling and then using an exhaustive search algorithm to enable the merger of multiple local 3D maps. The quality of these maps is such that the poses estimated by this method are accurate to within 0.1m and 1 degree.

Keywords. Mutual, Localization, Cooperative, Mobile, Robots, 3D, Mapping

1. Introduction

Extracting 3D information about the world surrounding a robot has proved difficult. The two main approaches, vision and laser range finding, have been dogged by problems. Vision is often computationally intensive and suffers from sensitivity to changes in illumination. Many of the difficulties stem from having to solve the correspondence problem which can be alleviated by structured light approaches, however the data spatial density does not come close to that provided by laser scanners. Non-visual localization and mapping has taken place in 2D, mainly due to limitations of the sensors in the case of laser range finders, or processor speed and algorithms for that of stereoscopic vision.

Recently in a drive to test the benefits of 3D sensors researchers have mounted 2D laser scanners on nodding or rotating mechanisms to obtain 3D scans [1,2]. Alternatively, two laser scanners mounted with their scan planes orthogonal [3] are also popular. The main problems with nodding or rotating approaches are difficulties in hardware implementation and high power consumption as the 2D scanners are heavy. Consequently a rotating mirror prototype has been built which produces 3D scans with a field of view of 100 by 180°, is light, has low power consumption and is easily deployed on conventional robotics platforms.

A number of groups are undertaking research into 3D laser mapping however very few groups are performing cooperative 3D laser mapping. The closest are groups using cooperative vision and laser based mapping in outdoor environments [4] and vision only [5]. The benefits of full 3D mapping are abundant and so the rapid expansion of this field is inevitable. The detection of negative and over-hanging obstacles greatly en-

hances avoidance behavior. Once 3D maps of environments have been built they can be customized for different robots. For instance various 2D occupancy grids may be built for robots of different sizes or with 2D sensors at different heights. Severely cluttered non-manifold environments such as search and rescue situations may be reliably mapped. Maps based upon the ceilings of rooms will remain accurate for longer and an unoccluded view of the ceiling is usually readily accessible to a robot even in crowded environments [6]. The disadvantages of 3D sensing technologies are slower acquisition time and the geometric increase in data that needs to be processed.

In this paper, the mutual localization approach discussed in Section 2.1 coupled with the 3D laser range finder prototype pushes this research into the new area of three-dimensional cooperative localization and mapping. Combining mutual localization with the data from multiple 3D laser scanners enables full 3D mapping of indoor environments. This would prove vital for a number of industries such as nuclear decommissioning, search and rescue scenarios, surveying as built structures and maps for mobile robots.

The rest of this paper is organized as follows. Section 2 presents the system framework of the research carried out in this paper. Section 3 details the 3D scanner hardware. Section 4 includes the experimental results and is followed by Section 5 discussing their implications along with future research directions.

2. System Framework

2.1. Mutual Localization

The premise for mutual localization is that rather than merely observing robots as beacons each robot observes and is itself observed simultaneously [7]. Additionally, ensuring that robots may observe team-mates and be observed themselves means that simultaneous mutual localization events can occur. These events allow superior relative pose determination. Firstly, the mutual localization is robust to spurious readings because simple checks on the validity of the mutual pose are available; for instance the separation of the robots should be similar as measured by both observing robots. Secondly, the accuracy in the pose does not deteriorate with separation, [7], a very useful property. Increasing separation merely decreases the frequency of mutual localization events. This is accomplished by mounting retro-reflective cylinders above the laser scanner as shown in Fig. 1(a). The 3D laser scanner prototype has a blind spot directly in front of it with an angular width of 20° thus higher mounted beacons will be visible from further afield. Most clutter in rooms is quite low, for example chairs and tables, so even when the line of sight between the robots is interrupted; the beacons, being some way from the ground, may still be detected by the laser scanners.

Mutual localization is accomplished by first projecting the observed beacon's 3D position onto the xy-plane which is parallel to the floor of the room. Once projected onto the horizontal plane the 2D mutual localization algorithm may be used. This method assumes that the beacons are always the same height above the floor, reasonable in the case for many indoor environments with flat horizontal floors. Given the relative pose of the mapping robot with respect to the observing robot multiple 3D laser scans may be combined to produce a local map.

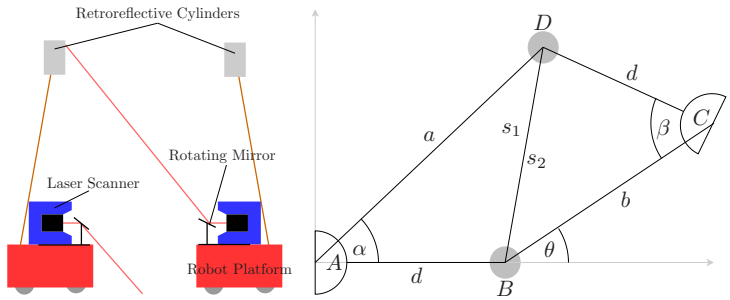

(a) (b)

Figure 1. Beacon positioning and geometry used to calculate the relative pose. AB is the stationary robot and CD the mapping robot. D and B are the beacons with C and D the origins of the laser scanners.

The beacons are above the laser scanner and there is a small horizontal displacement from the origin of the laser scanner. This displacement introduces the complications evident in Fig. 1(b), where the laser scanners are represented as semi-circles with the forward part of the scanner corresponding to the curve of the semicircle and the beacons as solid circles. The robots are at A and C, with C mapping whilst A remains stationary. The pose of A may be constrained to the origin and x-axis without loss of generality. The beacons, B and D, are attached to the robots at A and C respectively. The distances AB and CD are both equal to d. The separation of the beacons is labelled as s_1 and s_2 because s_1 is the separation as observed by the robot at A and s_2 is the separation as observed by the robot at C, which in practice will not be identical. The robot at A observes the beacon D at range a and angle α whilst that at C observes the beacon B at range b and angle β. The beacon separation may be calculated from the robot observations by the cosine rule for triangles. Comparison of the two values s_1 and s_2 (which should be approximately equal) allows erroneous localizations to be detected and rejected. Typical errors stem from distractors in the environment or error sensitive geometric configurations.

To acquire the position of the robot at C it is best to consider the geometry in the complex plane rather than the more immediately apparent geometric methods involving the sine and cosine rules. Using vectors in the complex plane gives two expressions for the position of C found by traversing the two available paths from the origin to C. A detailed explanation is given in [7]. Equating these gives the following expression for θ.

$$e^{\imath\theta} = \frac{ae^{\imath\alpha} - d}{b - de^{-\imath\beta}} \tag{1}$$

Eliminating $e^{\imath\theta}$ and simplifying gives C in terms of the observed angles, ranges and the parameter d.

$$C = \frac{abe^{\imath(\alpha+\beta)} - d^2}{be^{\imath\beta} - d} \tag{2}$$

The real and imaginary parts of C give the Cartesian coordinates of the second robot. The orientation is $\theta - \beta + \pi$ with θ determined from the argument of (1). The complex number calculations are done in Java using the Java Math Expression Parser (JEP) because Java does not natively handle complex numbers. The robots are able to exchange information

through wireless networking. Once the pose of robot C is acquired its scan data may be used to update the centrally held occupancy map.

The map is a standard occupancy grid [8], where each cell contains the probability that the particular space it represents contains an obstacle. The grid is initialized so that all cells contain 0.5 representing complete uncertainty. Typically the resolution is 0.1m and the size is 30 by 30m and the origin is the initial position of the observing robot. New sensor data is incorporated via the Bayesian update process described in (3). Occupancy grids are an effective map representation as they are robust, handle uncertainty well and allow fusion of data from different sensors [9].

$$P(\text{occupied}) = \left(1 + \frac{(1 - \text{evidence})(1 - \text{prior})}{\text{evidence} \times \text{prior}}\right)^{-1} \tag{3}$$

Due to the fidelity and narrow beam width of the laser scanner a straightforward raytrace model was employed. When updating the occupancy grid all cells along the path of the laser ray have their probabilities decreased whilst the cell containing the end point of the ray has its probability increased.

2.2. Global Localization

Whilst producing local maps in a cooperative manner, one of the robots remains stationary acting as a reference frame for building the map. In order to map areas larger than the local map the stationary robot must move at some point. This is an opportunity for odometry errors to adulterate the global map. Although these may be vastly reduced by moving the reference robot under observation of the mapping robot, these errors included at each step, albeit small, still undergo unbounded accumulation. Without some form of reference to the global map frame, mapping of large cyclic environments would prove impossible. Thus global localization is a necessity.

Usually mobile robots operate on the floor, consequently the 2D assumption may be enforced for global localization. In most typical indoor environments moveable objects tend to lie on the floor. Floor-level 2D maps (as most in previous 2D localization mapping research have been) are unreliable and quickly become out of date when furniture is moved and doors are opened or closed. To avoid these problems 2D map data is extracted as a horizontal cross-section just below the ceiling of the room. This volume of a room changes infrequently and is more easily observed especially in cluttered environments. The horizontal cross-section chosen was the volume from 2.3 to 2.9m in height and the resulting 2D occupancy grid is produced by simply summing the vertical columns within this height range and re-normalizing.

A plethora of global localization algorithms given a prior map exist however in this research an exhaustive search approach was implemented. This has a number of advantages, the entire pose probability density function may be recorded and inspected, it is very robust and suffers only from its slow execution speed. The impact of this on real-time operation may be vastly reduced especially if a position estimate is available which is almost always the case. The pose search algorithm may simply spiral search out from the estimated position. It was found that the execution speed of an unoptimized algorithm meant that global localization could take place on maps of size 20m by 20m with pose resolution of 0.1m and 1° in the order of minutes on a 2GHz processor. For the imple-

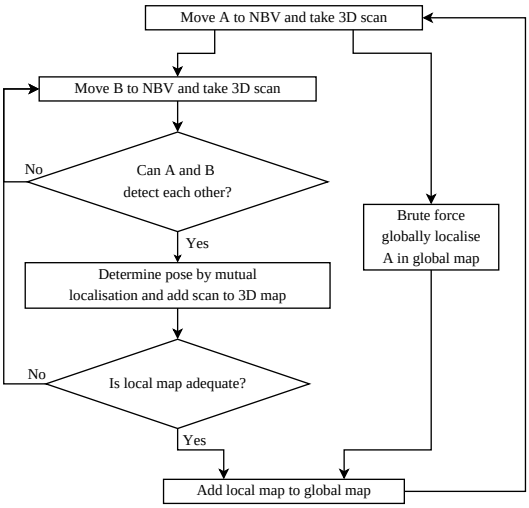

Figure 2. The 3D mapping process for two robots A and B

mentation of the exhaustive search algorithm the 3D sensor scanner is converted into a 2D occupancy grid by extracting the cross-section near the ceiling. A correlation metric is then calculated iteratively for the sensor occupancy grid by stepping through various poses with respect to the map. Typically, pose resolutions of 0.1m and 1° are used. The pose with the best correlation metric is then chosen. An example position probability distribution function is displayed in Fig. 5(b).

2.3. Concurrent Processing

Usually an exhaustive search algorithm of localization is unfeasible because it does not run fast enough to provide continuous real-time pose updates. However in this implementation the pose updates are supplied by the mutual localization. The global localization is run in parallel with the local map build process as depicted in Fig. 2. In Fig. 2 the first robot, A, moves to the next best view (NBV). The NBV is the next position which is most likely to yield useful observations for updating the map and in these experiment is calculated manually. Robot A is acting as the stationary robot providing a reference frame for B whilst B maps the local area around A. When the local map is sufficiently good it can be added to the global map. Whilst the local map around A's new pose is built the pose of A within the global map is calculated. This pose along with (3) enables the merger of the local and global maps. The process is repeated until the global map is of sufficient quality.

3. 3D Scanner Design

The 3D laser range scanner consists of a SICK LMS 200, rotating reflecting surface prototype (Fig. 3(a)) and software to convert the range scans into 3D data. The mirror rotation period is 40 seconds. The slow rotation speed contributes to a very low power consumption of 0.01W. Rotating at the same speed as the motor is the far blocking arm in Fig. 3(a). The purpose of this arm is to allow feed back of the angular velocity of the

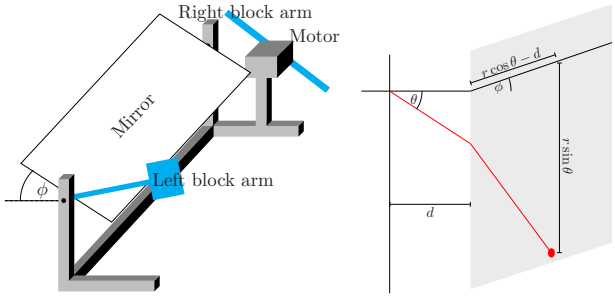

(a) (b)

Figure 3. Rotating mirror mechanism and calculating 3D coordinates from range data

mirror to the robot. This blocking arm approach circumvents problems synchronizing angular velocity with the laser data.

The laser scanner scans full 180° scans with most of the range data from side angles discarded. The furthest right hand scan points are blocked every half a second and this information is used to calculate the angular velocity of the motor and consequently the mirror. A particular advantage of this approach is ease of deployment in that the rotating mirror mechanism can simply be placed in front of the laser scanner and no further connections are required, even the power supply is self contained. The arm blocks are easy to detect as falling edges in the side range data.

The LMS was configured to scan a 100° arc at 1° intervals and mm measurement setting. These settings were chosen to minimize the number of scan points in order to increase the complete scan frequency. The scan frequency is limited by the data rate and at the moment is 0.05Hz. This data rate is 34.8kb/s, the maximum for the serial interface, resulting in 13 horizontal scans per second. The SICK LMS 200 can support a 500kb/s data rate using a USB interface. At this data rate, full 3D 1° by 1° scans should be possible at 0.5Hz.

The mirror is mounted in front of the scanner rather than rotating or nodding the scanner itself. This has a number of advantages namely less power consumption and simpler hardware setup. The disadvantages are a reduced scan angle to around 100°, a blind spot when the mirror is edge on and a requirement for more complex geometric calculations (Fig. 3(b)) to correct for the separation between the mirror and the scanner. In Fig 3(b) the effect of the mirror is to bend part of the xy-coordinate plane to a new elevation illustrated in grey.

The following equations, which reference the values indicated in Fig. 3(b), indicate the conversion between the r, θ and ϕ coordinates, measured by the laser scanner, and 3D cartesian coordinates.

$$x = ((r\cos\theta - d)\cos\phi + d, r\sin\theta, (r\cos\theta - d)\sin\theta) \tag{4}$$

where the value d is the separation between the origin of the laser scanner and the axis of the rotating mirror. The range and bearing as measured by the laser scanner are r and θ. The angle of the plane (grey region in Fig. 3(b) to the horizontal introduced by reflecting the laser ray from the rotating mirror in front of the scanner is indicated by ϕ.

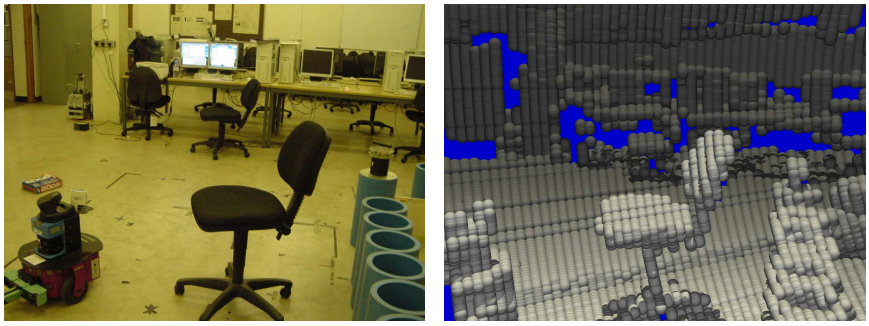

(a) (b)

Figure 4. Photograph and typical 3D scan of mapped room

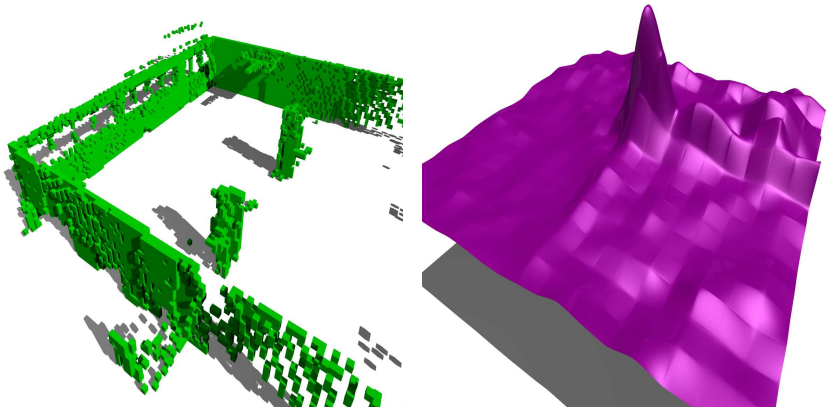

(a) (b)

Figure 5. Global sub ceiling map and position probability density function both with a resolution of 0.1m. The map is a thresholded occupancy probability grid of the space 1-2.9m above the floor. The width of the room is approximately 12m. Two pillars and the windows at the back are evident.

4. Experimental Results and Analysis

Results are visualized using a number of methods and software programs. To visualize the data a 3D scene is generated consisting of cubes or spheres representing occupancy and the results rendered using a ray tracer, Fig 4(b). This allows the production of high quality images and movies with shadowing, luminosity and perspective, visual cues that allow the brain to extract the 3D information more effectively from the 2D display media. However, despite these efforts it still remains difficult to effectively display 3D maps as images. An example of such a 3D image is displayed in Fig. 4(b) and a photograph from the corresponding view point is shown in Fig. 4(a). Each sphere in Fig. 4(b) represents a laser range return and is colored by its distance from the view point, with those closer being lighter.

Fig. 5 illustrates a typical global localization scenario; the occupancy grid, Fig. 5(a), is represented by drawing a cube at every grid cell where the probability of occupancy exceeds 0.9. Fig. 5(b) shows a postion probability density surface where the probability

of each position is indicated by the height of the surface. The reliability and accuracy of the pose may be ascertained by inspection of the position probability distribution. The true position is easily discerned and the dominance and shape of the peak denotes the reliability and error respectively.

5. Conclusion and Future Work

For decades mobile robots have been shackled by the 2D assumption, which has been necessary due to the absence of suitable 3D sensors. Even today 3D sensing technology is problematic and expensive. In this paper a rotating mirror mechanism has been added to a standard SICK LMS 200 laser scanner which produces 3D scans. These 3D scans coupled with mutual localization have produced full 3D environmental representations at very low cost. The fidelity of these representations has been validated by performing global localization within them.

Further work would include mounting the laser scanner so that it is facing up into the mirror to allow fuller scans which might allow localization by range histograms. Results from increasing the number of cooperating robots would be interesting. The 3D occupancy grids produced by mutual localization, although interesting for humans to inspect, will mainly be used by other robots. Thus the global localization accuracy is a good indicator of their fidelity and suitability for further use by other robots. Global localization in these maps delivers poses accurate to 0.1m and 1°.

References

[1] A. Nüchter, K. Lingemann, J. Hertzberg, and H. Surmann, "Heuristic-based laser scan matching for outdoor 6D SLAM," in *Advances in artificial intelligence. 28th annual German Conf. on AI*, Sept. 2005.

[2] K. Lingemann, H. Surmann, A. Nüchter, and J. Hertzberg, "Indoor and outdoor localization for fast mobile robots," in *Proceedings of the IEEE/RSJ Int. Conf. on Intelligent Robots and Systems*, Sendai, Japan, Sept. 2004, pp. 2185–2190.

[3] A. Howard, D. F. Wolf, and G. S. Sukhatme, "Towards 3D mapping in large urban environments," in *IEEE/RSJ Int. Conf. on Intelligent Robots and Systems*, Sendai, Japan, Sept. 2004, pp. 419–424.

[4] R. Madhavan and K. Fregene and L. Parker, "Distributed Cooperative Outdoor Multirobot Localization and Mapping," *Autonomous Robots*, vol. 17, pp. 23–39, 2004.

[5] J. Little and C. Jennings and D. Murray, "Vision-based mapping with cooperative robots," in *Sensor Fusion and Decentralized Control in Robotic Systems*, vol. 3523, Oct. 1998, pp. 2–12.

[6] W. Burgard, A. B. Cremers, D. Fox, D. Hahnel, G. Lakemeyer, D. Schulz, W. Steiner, and S. Thrun, "Experiences with an interactive museum tour-guide robot," *Artificial Intelligence*, vol. 114, no. 1–2, pp. 3–55, 1999.

[7] J. Ryde and H. Hu, "Laser based simultaneous mutual localisation for multiple mobile robots," in *Proc. of Int. Conf. Mechatronics and Automation*, Niagara Falls, Canada, July 2005, pp. 404–409.

[8] A. Elfes, "Using occupancy grids for mobile robot perception and navigation," *Computer*, vol. 22(6), pp. 46–57, 1989.

[9] P. Štěpán, M. Kulich, and L. Přeučil, "Robust data fusion with occupancy grid," *IEEE Transactions on Systems, Man and Cybernetics*, vol. 35, no. 1, pp. 106–115, 2005.